Results in Engineering 25 (2025) 104112

Contents lists available at ScienceDirect

Results in Engineering

journal homepage: www.sciencedirect.com/journal/results-in-engineering

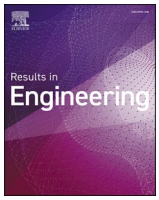

Research paper

Effective rain rate model for analysing overestimated rain fade in short millimetre-wave terrestrial links due to distance factor

Asma Ali Budalal [a,*], Ibraheem Shayea [b,c], Md. Rafiqul Islam [d], Jafri Din [e], Abdulsamad Ebrahim Yahya [f], Yousef Ibrahim Daradkeh [g], Marwan Hadri Azmi [h]

[a] Department of Telecommunication and Electronics Technology, College of Electrical and Electronic Technology Benghazi, Libya
[b] Electronics and Communication Engineering Department, Faculty of Electrical and Electronics Engineering, Istanbul Technical University, Sarıyer 34467, Turkey
[c] Department of Intelligent Systems and Cybersecurity, Astana IT University, 010000 Astana, Kazakhstan
[d] Department of Electrical and Computer Engineering, International Islamic University Malaysia (IIUM), Gombak, 5072 Malaysia
[e] Wireless Communication Centre, Faculty of Electrical Engineering, Universiti Teknologi Malaysia (UTM), Johor Bahru, 81310, Malaysia
[f] Department of Information Technology, College of Computing and Information Technology, Northern Border University, Arar, Saudi Arabia
[g] Department of Computer Engineering and Information, College of Engineering in Wadi Alddawasir, Prince Sattam bin Abdulaziz University, Al-Kharj 16273, Saudi Arabia
[h] Wireless Communication Centre, Faculty of Artificial Intelligence, UTM Kuala Lumpur, 54100 Kuala Lumpur, Malaysia

ARTICLE INFO

Keywords:
Effective rain rate
Predicted rain fade
Distance factor
Short-length
Millimetre-wave
Terrestrial Links

ABSTRACT

Significant discrepancies have been observed between the measured attenuation induced by rain over mm-wave terrestrial links at very short communication paths and the predicted measurement by ITU-R P.530-18. Recent observations indicate that the rain rate at 0.01 % occurrence used by the ITU-R prediction method does not represent effective rain intensity for less than 1 km of path length, despite its accuracy for paths longer than 1 km. These deviations can be attributed to several factors, such as spatial inhomogeneity, rain cell diameter, and environmental variations. Additionally, sudden changes in the propagation environment, such as wind direction, humidity, and wind speed, contribute to non-uniform rain distributions. Additionally, there is still a lack of comprehensive investigations due to the involved experimental difficulties. Thus, an effective rain rate concept and model are proposed to represent rain intensity variations for short paths to eliminate the need for an effective path length that more accurately predicts rain attenuation at path lengths exceeding 1 km. The proposed model is based on the measured $R_{0.01\ \%}$, short path (less than 1 km) and frequency. Two-year measurements of both the rainfall rate and rain attenuation over two experimental links operating at 26 and 38 GHz at a 0.3 km path length are used to validate and enhance the model. The measurements and experiments are conducted in Malaysia. The result indicated that the shorter the link, the higher the expected R_{eff}. One aspect that may partially justify this significant increase in R_{eff} is the fact that the ITU-R P.838-3 model does not consider the impact of the raindrop size distribution (DSD)for tropical climates when predicting rain attenuation at a short-range mm-wave link. The proposed model estimations are compared with experimental attenuation results reported at 73.5GHz and 83.5GHz over a 0.3 km path length. Several experimental results reported from different regions around the globe are used to validate the proposed model. The outcomes are in good agreement. The findings emphasize the importance of developing region-specific models that consider local meteorological variations, potentially offering significant improvements to the reliability and design of mm-wave communication systems and realizing the future goal of 6G wireless mobile fronthaul.

1. Introduction

The emergence of innovative applications such as artificial intelligence (AI), virtual reality (VR), three-dimensional (3D) media and Internet of Things (IoT) networks is expected to significantly increase mobile traffic over the next decade. The forthcoming generation of cellular networks (6G) faces the challenge of handling massive data volumes while providing high-data-rate connectivity per device. This is

* Corresponding author.
E-mail addresses: asma.budalal@ceet.edu.ly (A.A. Budalal), ibr.shayea@gmail.com (I. Shayea), jafri@utm.my (J. Din), y.daradkeh@psau.edu.sa (Y.I. Daradkeh).

https://doi.org/10.1016/j.rineng.2025.104112
Received 2 December 2024; Received in revised form 11 January 2025; Accepted 20 January 2025
Available online 21 January 2025

anticipated since the higher throughput of backhauling links will aggregate traffic from several users [1]. With a large number of registered users and their demand for high-quality multimedia content, the millimetre-wave system enables greater data transmission rates between the gateway and small-cell base stations, thereby enhancing the overall system throughput [2]. To break the spectrum gridlock and to dramatically expand system capacity for the evolving 5G and 6G mobile networks, millimetre-wave technology using small cells will play a crucial role in achieving the envisioned network performance and communication tasks [3].

According to the latest report produced by Ericsson [4], 40 % of global wireless backhaul systems are expected to be based on microwave technology by 2023.

The latest WRC-19 document [5] states that 24–86GHz bands will be treated as candidate frequencies for 5G applications. While waiting for the finalisation of 5G regulations and specifications for different scenarios and applications, several countries have already implemented commercial 5G systems with a particular focus on the frequency range of 26.5–29.5GHz [6].

Ultra-reliability of 99.999 % is the fundamental aim of the 5G system in order to effectively support several sophisticated applications such as industrial control, healthcare and vehicle-to-vehicle (V2V) communications [1]. However, mm-wave technology is challenging due to propagation sensitivity [6,7]. The path losses are generally much higher at 30–300 GHz, even at short communication distances of 200 m [2]. To meet the channel requirements of future 6G communication networks, the channel must be measured to assess the path loss, multi-band, fading, blocking effect, multipath clustering as well as transmitter and receiver movement speed, direction and time. Additional losses, such as foliage attenuation and off-body fading, must also be considered. The weather effects on outdoor radio propagation, such as atmospheric absorption, rain, snow, fog and dust, are also significant in the implementation of mm-wave and sub-THz wireless systems [6–12]. These technical challenges must be resolved to fully exploit the application potential of small-cell mm-wave topologies for outdoor networks since they are the enabling technology for future communication networks. With strategic deployment over short distances, they can overcome the limitations of signal attenuation and ensure coverage in dense urban environments.

Overcoming attenuation from weather effects is possible for mm-wave and sub-THz radio propagation channels with the use of high-gain directional antennas or antenna arrays at TX and RX with numerous dB gain and small cell technology [1,7,8],. However, rain-induced attenuation cannot be neglected, even for a small cell size radius, to effectively achieve ultra-reliability requirements of outdoor scenarios in tropical climates [13–18].

Rain attenuation at the millimetre wave is progressively more influenced by the Drop Size Distribution (DSD) [19]. The wavelength has the same dimension as the raindrop diameter and becomes comparable to small and medium-sized raindrops. These smaller drops exhibit stronger Mie scattering, which can lead to increased attenuation compared to Rayleigh scattering at lower frequencies. The relative contribution of small and medium-sized drops to the total rain attenuation increases with higher frequency [19].

The necessity for more robust rain fade prediction models for small-cell designs is currently the main issue. Improving the accuracy of prediction models can provide a means to define the behaviour of mm-wave propagation channels over short distances. This can offer enough information on path loss modelling, link budget calculation and channel propagation characteristics at very short paths throughout various climatic regions [20–22]. However, the effects of precipitation on short links have not been thoroughly investigated, especially in tropical regions. Hence, an accurate propagation prediction model for short-range millimetre-wave links that considers different scenarios is necessary. This will provide precise information on antenna and power transmission requirements, transmitter and receiver designs as well as interference levels which will aid in the development of ultra-reliable systems for outdoor applications [23]. This paper provides accurate predictions of rain attenuation for the design of millimetre-wave terrestrial links over a short communication path.

2. Background

In tropical climates, high rain rates that reach up to 270 mm can influence the propagation channel and ultra-reliability requirements of outdoor applications as compared to temperate regions. When using the NYUSIM channel model for outdoor environments [24–26] with measured data at 38 GHz, the propagation channel's behaviour is severely affected by heavy rain at 125 mm/h. In Malaysia, the received power decreases by more than 15 dB on a 300 m link at 38 GHz due to higher path loss during rain. However, these results are based on one-month measurements at a fixed path length. The random temporal and spatial variations of rain at a short distance, especially in tropical regions with the convective rain type, may further indicate that raindrops merge and result in highly significant absorption and scattering processes [27].

Based on conducted measurements over the propagation path of more than 1 km, the effective path length multiplied by the specific attenuation can be obtained from the rain rate distribution along the propagation path using the power-law relationship, which provides an accurate estimation of rain fade [28,29]. In this regard, most existing prediction models will 'average out' the spatial inhomogeneity of the rain rate that is uniformly distributed over the propagation path and defined as specific attenuation calculated per unit of distance (dB/km) [30–34]. In [22], the prediction model applies the effective rain rate concept, however, it may provide inaccurate predictions of the effective path length for distances below 700 m [22].

Generally, specific attenuation (dB/km) is a powerful theoretical source for predicting rain attenuation at path lengths exceeding 1 km. Based on conducted measurements at 26GHz along 1.3 km in Malaysia and 38 GHz along 3.2 km in Korea, it has been found that the rain attenuation predicted by ITU-R can provide a fade prediction similar to the measured one for path lengths exceeding 1 km [25,35,36]. However, a significant difference has been recorded between the measured and estimated rain attenuations using the ITU-R P.530 prediction model over a short-range Los link [28,29,37–41]. These deviations can be interpreted as: (i) the spatial inhomogeneity of the actual rain along the path, especially over a short path length, (ii) the rain cell diameter must be considered more than the distance reduction factor at higher frequencies (the two concepts are strongly related since a small cell will correspond to a decrease in the path reduction factor and vice versa) and (iii) the sudden variations in the propagation environment include changes in wind direction, humidity, wind speed, etc. [39]. Wind direction can affect the distribution of rain along the propagation path, leading to non-uniform rain rates. This can affect the accuracy of the path reduction factor used in calculating attenuation. Humidity levels can influence the condensation and evaporation of raindrops, affecting the rain rate and drop size distribution. These changes in rain characteristics can lead to varied attenuation coefficients (k and α). Wind speed can alter the trajectory of raindrops and the overall rain distribution along the link. This can influence the assumptions made in the effective rain rate technique, leading to discrepancies between the predicted and actual attenuation.

From the experimental and theoretical prediction models, systematic deviation is attributed to the wet antenna attenuation effect [28,29,40,38]. The specific attenuation's mathematical formula in ITU-R P.530 [34] already accounts for the spatial inhomogeneity of the rain rate along the path (the path reduction factor). Additionally, the DBSG3 database employed to fit the model's coefficients also contains data for links shorter than 1 km. The latest modifications to the ITU-R P.530 model have been explicitly conducted to fit these measurements.

In this approach, the effective path length (d_{eff}) is calculated from the

product of the actual path length and the path reduction factor, which considers three input parameters: the actual path length, $R_{0.01\ \%}$ and the operating frequency. However, we need to interpret the deviation between the predicted and measured rain attenuation over the short-range path. The ITU-R P.838-3 model does not consider the impact of the drop size distribution (DSD), which for tropical climates and high frequencies, can be more pronounced compared to temperate climates and low frequencies. The wet antenna effect leads to increased signal attenuation caused by water droplets accumulating on the surface of the antenna. This water layer can absorb and scatter the transmitted or received electromagnetic waves, leading to additional signal losses beyond the attenuation caused by the rain itself. In this regard, we must describe the rain-induced attenuation over short-range millimetre-wave terrestrial links, taking into account the effects of wet antenna and DSD.

The experimental data analysis of the most extreme rain events in various climate regions has indicated that during convective downpours, the rain rate may not have consistent distribution along the path, even in the case of very short links [31]. Thus, specific attenuation within the cell significantly differs on a short path since rain cell sizes may vary according to the location of the conducted measurements. For short communication paths, it is assumed that the effective rain rate that can induce attenuation will be relatively higher than the average rain intensity within the 1 min integration time of the rain cell proposed by the ITU-R Model. Thus, the peak rain rate increases within a short path [40]. The path reduction factor of that model significantly changes as a function of the path length, even more so for $d < 1$ km. Therefore, it is recommended that the R0.01 % rain rate should be modified to an effective rain rate in ITU-R P.530-17.

None of the mentioned studies had modified the existing rain attenuation models to predict rain fade at very short mm-wave terrestrial links, especially in tropical areas with intense rainfall rates. The most recent investigation by Budalal et al. [25] was of the distance factor behaviour in ITU-R P530.17. It was found that the distance factor values are inconsistent for path lengths less than 1 Km. The results in [25] presented the increment factor as an alternative to the path reduction formulation in rain attenuation prediction for short-range millimetre-wave links. Therefore, the distance factor in ITU-R P.530-17 was modified.

Accurate rain attenuation prediction models with higher efficiency at short terrestrial microwave links are vital for designing and optimising mm-wave systems. This paper presents methods for predicting rain attenuation necessary for designing terrestrial line-of-sight systems over short-path millimetre-wave links under 1 km, incorporating and validating the effective rain rate (R_{eff}) model. Propagation data at 26 and 38 GHz have been collected over a two-year period in Malaysia. Several measurements are considered for various locations and extremely short mm-wave links have been utilised for model validation.

3. Data and methodology

The rain intensity and rain attenuation were simultaneously measured at 26GHz and 38 GHz for a short-range path length of 300 m [42]. The calculations took place at the wireless communication centre (WCC) of the University of Technology Malaysia. The University of Technology Malaysia (UTM) is located in Johor Bahru, Malaysia. The general coordinates are approximately 3.1616° N latitude and 101.6869° E longitude. Johor Bahru has a tropical climate, which is hot, humid and wet throughout the year. Temperatures are consistently warm, with average daily temperatures ranging from 25 °C (77°F) to 34 °C (93°F). Humidity is high, typically between 70 and 90 %. Johor Bahru experiences significant rainfall with an average annual precipitation of around 2500 mm (98 inches). The region has two main seasons: a wet season from November to January, and a slightly drier season from June to August. Thunderstorms and heavy downpours are common, especially during the wetter months. In Malaysia, the tropical climate leads to intense and often localized rainfall events, which can result in higher rain rates and variability. The characteristics of rain in this region, such as the drop size distribution (DSD) and the frequency of heavy rainfall, contribute to significant path loss, particularly at higher frequencies like 38 GHz. Fig. 1 presents the experimental system diagram. The time availability of rain attenuation measurements on MINI-LINKS 38E and 26E (manufactured by Ericsson) is 98.6 % and 99.5 %, respectively. Table 1 highlights the specifications of both links in more detail.

3.1. Extraction of rain rate data from Casella rain gauge

The Casella tipping bucket rain gauge, shown in Fig. 2, is used in applications that include hydrology, rainfall monitoring, rainfall distribution and intensity, remote monitoring, run-off monitoring, ecological studies, agriculture as well as climate change studies. The bucket size accommodates heavy rainfall (0.5 mm). It is fitted with a solid-state logger. Only the number of tips is counted and stored in the battery-operated micrologger cassette. This implies that the one-minute rain rate will be read as a multiple of 30 mm/hr. Its long-term data is very useful in obtaining reliable statistics. A MATLAB program based on an algorithm is utilised to convert the recorded tipping time into one-minute rain rate data. The algorithm applies the assumption that the rain rate is uniform between two consecutive tips if the time difference is not more than two and and each tip represents 0.5 mm. The program was previously developed by Chebil [41] and later modified by the researchers who further calibrated Casella RG. Calibration was conducted in the laboratory within the specified ±5 % accuracy of the equipment.

3.2. Accuracy of Casella RG with rainfall intensity

Casella has three types of tipping bucket rain gauges with 0.1 mm, 0.2 mm and 0.5 mm sensitivity. For medium and high rainfall rate, the 0.5 mm sensitivity rain gauge provides better accuracy than the 0.1 mm and 0.2 mm rain gauges. For rainfall intensity ranging between 150 mm/h to 200 mm/h, the errors encountered by the 0.5 mm rain gauge is about 3 %. During measurements, the 0.2 mm and 0.1 mm rain gauges produced errors of 5 % and 15 %, respectively. For the Malaysian tropical climate, the rain gauge with 0.5 mm sensitivity is more suitable.

3.3. Time availability of rain rate data

For reliable statistical results, the collected rain data should have an availability greater than 90 % for each year [42]. Since the data must be continuous, it should be carefully selected to obtain maximum availability during each year. Casella is a compact unit equipped with inside batteries that function with 100 %-time availability for most of the years. The Casella rain gauge measures the rain rate with one minute integration time. The cumulative distribution is obtained by computing

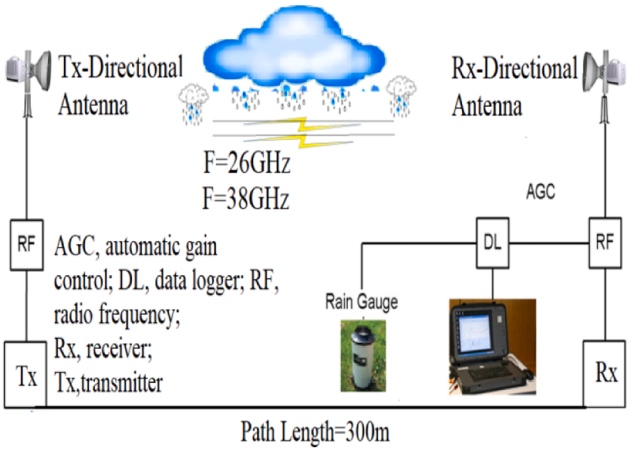

Fig. 1. Illustration of the experimental setup block diagram [41].

Table 1
Specifications of mini links.

Descriptions	Link1	Link2
Frequency Band	26GHz	38GHz
Path length	300m	300m
Polarisation	HP	HP
Antenna Gain	41.0 dBi	44.9 dBi
Antenna type	Directional	Directional
Maximum Tx Power	18 dBm	15 dBm
Link length	300m	300m
Availability	98.6 %	99.5%
Tx Antenna height	17.3 m	17.3m
Rx Antenna height	18.7m	18.7m
Value of threshold (dBm)	−36.2	−25.3

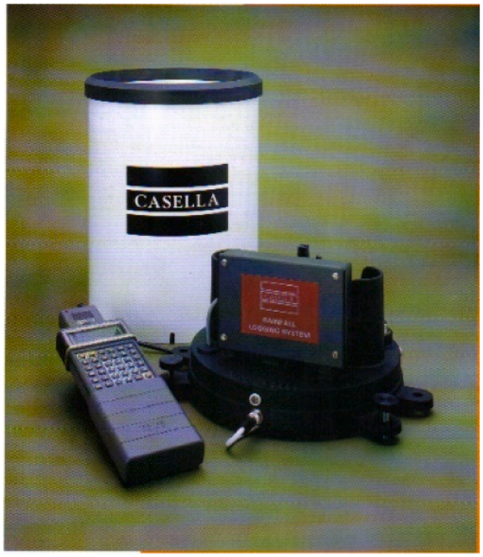

Fig. 2. Rain rate data logging system (Casella).

P ($R \geq$ rt) which is the probability that one-minute rainfall intensity R (mm/h) exceeds a threshold value rt (mm/h) for a time period T. It has been formulated by Chebil et al. as:

$$P(R^3 rt) = Nt/NT \quad (1)$$

where Nt is the number of rain rate data larger than rt and NT is the total number of minutes in time period T. The MATLAB program calculates the cumulative distribution from the measured rain rate. The Casella rain gauge can only produce the discrete value of the rain rate which is a multiple of 30 mm/h. Since the Casella rain gauge cannot record rain rates less than 30 mm/h, larger errors are expected if the threshold value of rt (mm/h) is set to start from 30 mm/h. With careful selection, a threshold value for rt was proposed by Chebil [41] as follows:

$$rt = r0 + 30n \quad (2)$$

where n is a positive integer and r0 = 15 mm/h.

Fig. 3 displays the cumulative distribution of data for one year based on the one-minute average rain rate and the number of tips per minute. The cumulative distribution of data was measured from January 1998 to December 1999. Fig. 3 presents the daily measured rain rate, while Fig. 4 highlights the monthly CCDF (Complementary Cumulative Distribution Function) rain rate in mm/h. Fig. 4 demonstrates how the monthly CDF (Cumulative Distribution Function) of rainfall intensity is influenced by the southwest monsoon from April to September and the northeast monsoon from October to March. The rain rate was collected each month, and an average graph was plotted for the entire year, as shown in Fig. 5. The annual distribution of rain rate CDF for the same

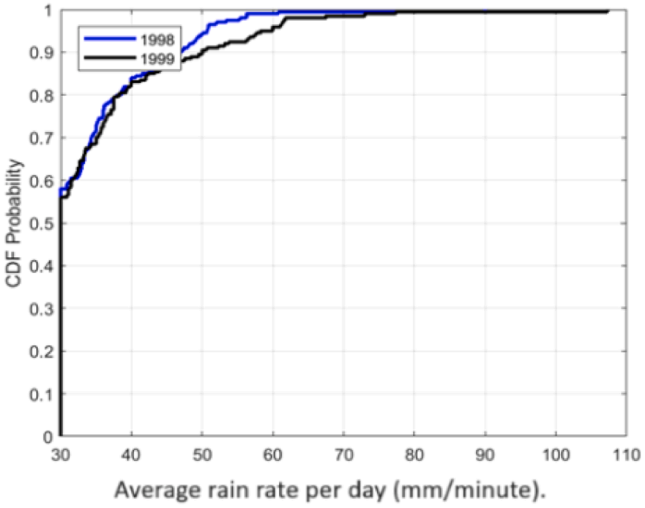

Fig. 3. The daily average rain rate in Malaysia.

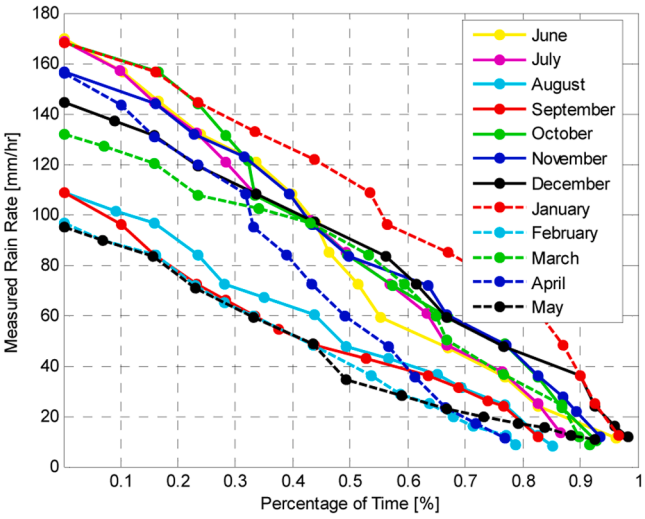

Fig. 4. Monthly CCDF measurements of rain intensity in Malaysia.

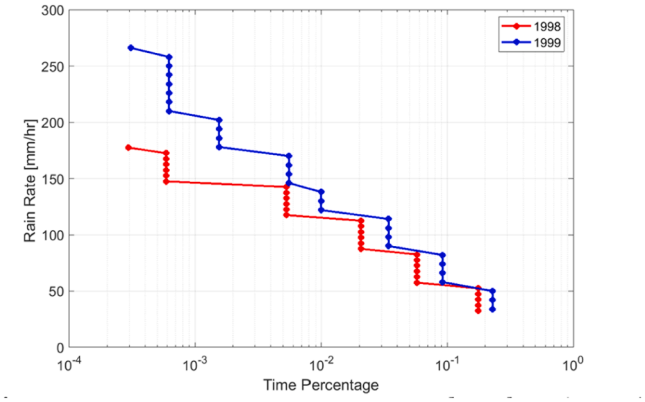

Fig. 5. Two-year measurements presented as the rain rate's cumulative distribution function.

areas varies from year to year, as demonstrated in Fig. 5. The rain rate exceeds 150 mm/h at lower fractions of time ($P < 0.01$ %). The presented results indicate that the monthly rain rate shifts between 58 mm/hr to 136 mm/hr at 0.01 % of time, whereas the average yearly rain rate

comes to 125 mm/h. From previous investigations [36] performed in the same area at Universiti Teknologi Malaysia (measured from June 2011 to May 2012), the recorded rain rate $R_{0.01}$ was 120 mm/h. From the CCDF graph in Fig. 6, the measured rain rate is almost similar for the same location at $R_{0.01}$.

3.4. Rain attenuation measurements

The total number of minutes during rain is 6341 out of 139 rain events throughout one year. Rainfall intensity data is collected with a 1-min integration time. In contrast, the received signal strength is organised with a sampling period of (1 s) resolution. Next, the rain attenuation data is processed by applying the 1 min average period. The processed date is then plotted to form a continuous rain curve, which may be considered accurate above the 30 mm/h rainfall rate. The reason behind this has been discussed in Section 3.3. The received signal variations during rain events are obtained from the 38 GHz wireless link shown in Fig. 6. As seen in the figure, the RSL (dBm) fluctuates around −25.5 dBm in clear sky conditions. However, after rain, it sharply drops to −64.5 dBm, which corresponds to the highest rainfall rate (270 mm/h). A data acquisition card (PCL 818) is installed with a personal computer to interface and log the automatic gain control (AGC) from the RF unit. The AGC level is sampled every second and set at a selected threshold level in the event of rain. The data is recorded every second below this level. For non-rainfall events, the AGC level is averaged and recorded every minute. The signal level varies from −25.3 dBm to −61.6 dBm for the 38 GHz link and −36.2 dBm to −70.5 dBm for the 26GHz link, respectively. A wooden box is installed to protect both antennas from moisture effects during measurements, which helps achieve accurate results. Although the wet antenna effect is not present, the wooden box did become wet, causing an issue similar to the wet antenna effect. Extracting the rain attenuation level from the RSL by imposing a fixed threshold will not allow isolating the impact of rain on the link; therefore, the wet antenna/box effect will not be removed. The RSL level just before and after the rainfall event has been considered in order to only extract the rain attenuation. The rain event is identified by examining the concurrent rain gauge measurements. When the rain stops, the RSL may not promptly return to its clear sky value due to the wet antenna/box effect.

3.5. Measurements and ITU-R predictions

The fade due to rain for the 0.01% exceedance probability, denoted as $A_{0.01\%}$ (dB), can be calculated using the formula provided in ITU-R Recommendation 530-18. This formula estimates the attenuation caused by the terrestrial line-of-sight (LOS) link due to rainfall as follows:

$$A_{0.01} = g d_{ef_f} = \mathrm{k}\, \mathrm{R}_{0.01}^{\alpha} dr \quad dB \tag{3}$$

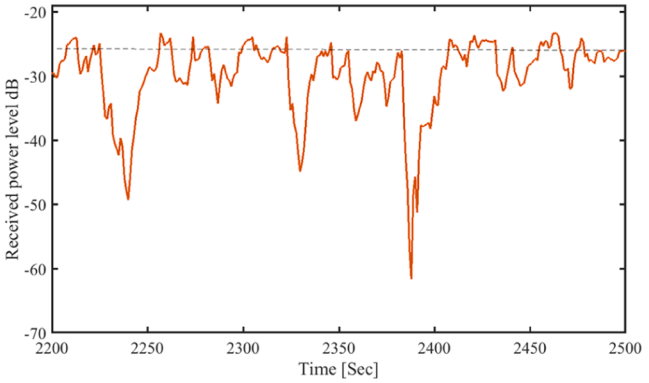

Fig. 6. Received signal variation at 38-GHz observed during a rainfall event.

where specific attenuation, the effective path length and rain rate at 0.01% are expressed as γ (dB/km), d_{eff} and $R_{0.01\%}$, respectively. The values of regression coefficients k and α for different frequencies are found in ITU P.838-3, the propagation path length is d and the distance factor r is defined as:

$$r = \frac{1}{0.477 \mathrm{d}^{0.633}\ \mathrm{R}_{0.01}^{0.073\alpha}\ \mathrm{f}^{0.123} - 10.579(1 - \exp(-0.024\ \mathrm{d}))} \tag{4}$$

where the frequency f is in GHz, the propagation path length is d in km and α is the same as in Formula (3). The following expressions, from (5) to (9), are proposed to estimate the total attenuation A_p for $p = 0.001\%$ to 1%:

$$\mathrm{A_p} = \mathrm{A_{0.01}}\ \mathrm{C_1}\ \mathrm{p}^{-\left(\mathrm{C_2} + \mathrm{C_3}\ \log_{10}\mathrm{p}\right)} \tag{5}$$

with:

$$\mathrm{C_1} = \left(0.07^{\mathrm{C_0}}\right)\ \left\lfloor 0.12^{(1-\mathrm{C_0})} \right\rfloor \tag{6}$$

$$\mathrm{C_2} = 0.855\ \mathrm{C_0}\ + 0.546\ (1 - \mathrm{C_0}) \tag{7}$$

$$\mathrm{C_3} = 0.139\ \mathrm{C_0}\ + 0.043\ (1 - \mathrm{C_0}) \tag{8}$$

where:

$$\mathrm{C_0} = \begin{cases} 0.12\ + 0.4\ \left[\log_{10}(\mathrm{f}/10)^{0.8}\right] & f \geq 10\ GHz \\ 0.12 & f < 10\ GHz \end{cases} \tag{9}$$

The rain fade measured over two years is used to construct complementary cumulative distribution (CCDF) at 26 GHz and 38 GHz, as shown in Fig. 7. The same predicted by ITU-R P.530-17 [34], Mello Da Silva [32], Abdelrahman [43] and Ghiani [31] are also compared in Figs. 8 and 9. The models of Abdelrahman and Ghiani underestimate the measurement, while the models of Silva and ITU-R P.530–17 significantly overestimate the measurement. Observations have confirmed these results, as presented by Lam et al. [14,27]. The outcomes indicate that the ITU-R model overestimates attenuation for all examined locations, particularly for extremely heavy rainfall ($R > 100$ mm/h). The overestimation becomes high for 0.01% or 0.001% exceedance of time. This observation agrees and confirms with the results presented by Valtr et al. [40,35,38,39,37,44]. In [27], the unreasonably high attenuation values predicted by the Silva model in Brazil are justified since the model is valid until approximately 700–800 m. Ghiani's model performed better at exceedance probabilities of around $P \geq 0.02\%$ (mostly at low rain intensity).

The distance factor applies to various link geometries, from short-range to long-range links. The distance factor in the formula helps model this spatial distribution of rainfall and its impact on the overall

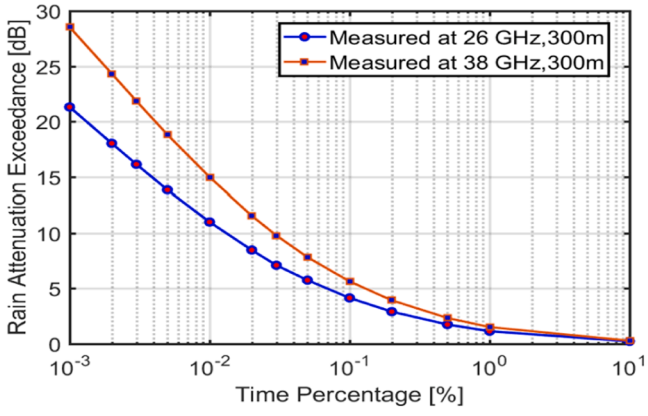

Fig. 7. Measured two-year rain attenuation probability distributions over the 26GHz and 38 GHz links.

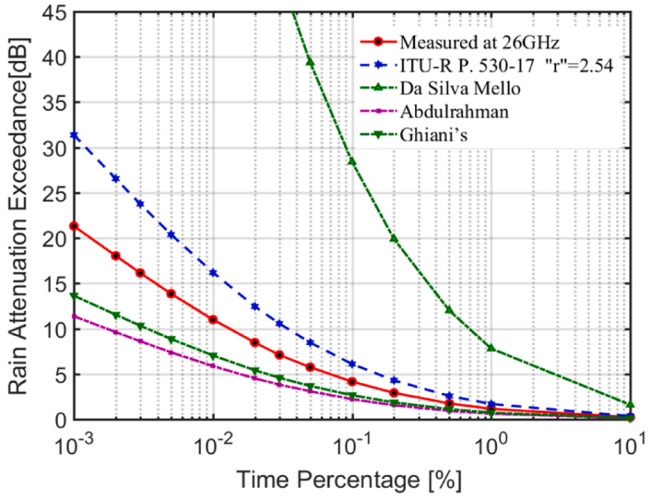

Fig. 8. Comparison between measured rain attenuation at 26GHz and those predicted by other models.

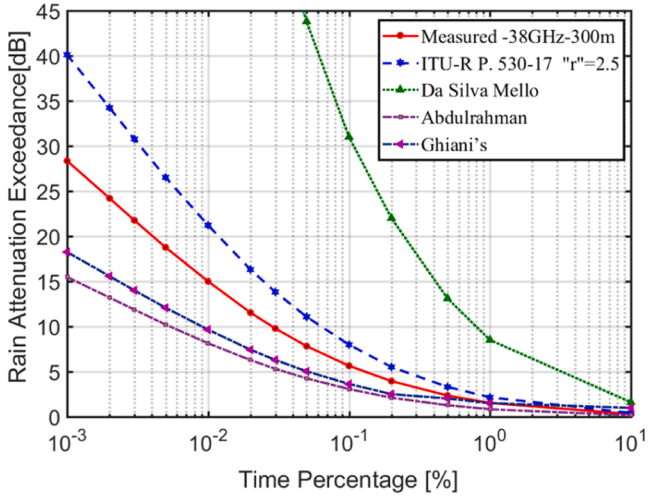

Fig. 9. Comparison between measured rain attenuation at 38 GHz and those predicted by other models in [31,32,34,43].

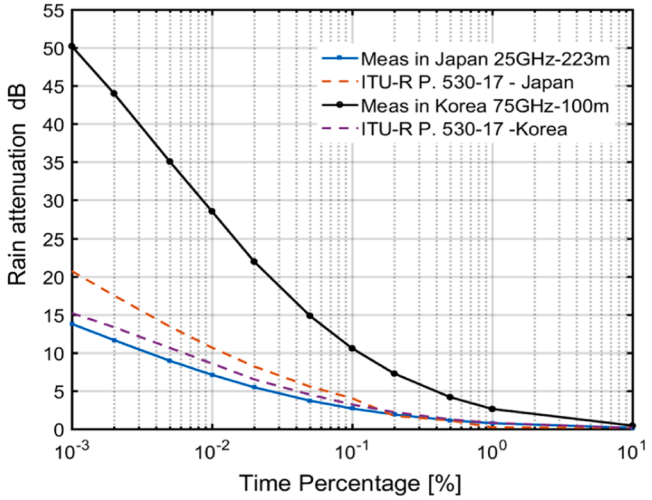

Fig. 10. Comparison between measured attenuation at 75GHz [35] and 25GHz [45] with those predicted by ITU-R P.530-17.

attenuation. Fig. 10 displays the ITU-R 530–17 model's inability to predict rain fade at 75GHz for 100 m link in Korea and at 25GHz for 223 m link in Japan [35,45]. It is also apparent from Figs. 8–10 that the recommended distance factor is not suitable for short-range links [38, 39,46,47]. Note that the local data in Fig. 5 are used as inputs for the models.

The same phenomenon was observed by Al-Saman et al. [18] at 21.8 GHz and 73.5GHz over distances of 1.8 km and 0.3 km in Malaysia. The predicted rain attenuation values entirely align with the ITU-R attenuation for the 1.8 km link at both frequencies. However, the ITU-R P.530-17 model is inaccurate for the 300 m link, showing discrepancies at time percentages from 0.01% to 1% with a maximum distance factor of 2.5, as stated in [18].

From Eq. (12), the factor r is inversely proportional with (f, d and $R_{0.01\%}$). Extensive investigations revealed that r slightly varies from f, but mainly with $R_{0.01\%}$ and d. Moreover, the distance factor r is significantly affected by α when the path length $d \geq 0.96$ km. We suggest that the value of α should be ignored since in ITU-R P.838-3, the variation of the α coefficient at vertical and horizontal polarisations is very slow for the mm-wave frequency range. The dependency of r on d is significant since it is empirically derived from a wide range of terrestrial LOS link geometries, from short-range to long-range links. This ensures that the formula can be used for accurate rain attenuation estimation across different link configurations. Short link data is present in the DBSG3 database, however, the accuracy at short paths still requires improvement.

The path reduction factor in terrestrial links is a key criterion to efficiently compare the performance of different rain attenuation models [30,43]. The path reduction factor sharply rises past 1 for links with less than 2 km path length.

The current prediction models assume that d_{eff} values are longer than the actual path length in a very short communication path. However, this concept is logically unacceptable since ITU-R has established the specific rain attenuation formula as dB/km, which is globally accepted and found to be accurate in path length > 1 km. The distance factor r in the ITU-R model [34] considers the rain rate heterogeneity along the propagation path as well as the rain cell distribution and frequency of operation (d, $R_{0.01}$, f).

The distance factor exceeds 2.5 when the actual path length is at a range of 300 m [28,29]. Therefore, the current parameters of ITU-R P.530-17 must be re-evaluated to successfully apply to very short path lengths at different climatic regions. By utilising the measured one-minute rain rate and by knowing the behaviour of the received signal strength during rain, the actual rain rate can be calculated according to ITU-R [27,48] as:

$$R_{0.01\%} = \left[\frac{A_{0.01\%}}{d.r.k}\right]^{\frac{1}{\alpha}} \quad (mm/h) \tag{10}$$

The rain intensity value can be derived from the corresponding attenuation data by using the distance factor r and the link's other parameters, as given in Eq. (10). The conversion can be considered as the inverse of Formula (9) [13]. It should be noted that the rainfall rate for 0.01% exceedance of time during an average year ($R_{0.01\%}$) measured from a real-time rain gauge may not accurately reflect the rain-induced attenuation over short-range links. Rain intensity estimation using a short time interval is more likely to follow the instant changes and dynamics of rain events and monitor the peak rain rate. This indicates that the rain rate derived from rain attenuation data can represent an accurate rain rate for a short path compared to the measured rain rate obtained from the rain gauge. At 0.01% exceedance of time, the rainfall rate was around 125 mm/h, while the value obtained from the measured rain attenuation using Eq. (9) is 240 mm/h (considering that $r = 1$). Due to the assumption of uniformly distributed rain intensity along the path, as proposed in [23,24], a path reduction factor has been set to 1 for the path length < 1 km.

We have thoroughly investigated the relationship between γ (which is the theoretical specific rain attenuation obtained from ITU-R P.838-3), as presented in Formula (9), and γ_{eff} (which represents the specific rain attenuation along a short path obtained from the measured total attenuation), as presented in Eq. (11).

$$\gamma_{eff} = \frac{A_{Measured}}{300} \times 1000 \text{ dB} \Big/ \text{km} \tag{11}$$

Due to the assumption of uniformly distributed rain intensity along the path, as suggested in [23,24], a path reduction factor has been proposed to equal to 1 for the path length < 1 km. However, the conducted experiments in this paper reveal that the relationship between γ and γ_{eff} must be thoroughly investigated.

4. Concept of specific attenuation increment factor $I_{f\gamma}$

In this section, the increment factor ($I_{f\gamma}$) is proposed instead of the conventional reduction factor since it is valid for long-range links. The increment factor is assumed to interpret the increasing trend of γ_{eff} (measured) and γ (predicted by ITU-R).

The increment factor of the rain rate is derived in [25] based on the actual radio link length (d < 1 km), frequency (f GHz) and one-minute rain rate ($R_{0.01\%}$). This work highlights the Increasing Factor (I_fγ) defined in (12) and proposes that if the link is shorter than the rain cell diameter, the effective path length matches the link length:

$$\frac{\gamma_{eff}}{\gamma} = \frac{k\, R_{eff}^{\alpha}}{k\, R_{0.01}^{\alpha}} = I_{f\gamma} \tag{12}$$

where $I_{f\gamma}$ is the increment factor of the rain rate that causes variations between the measured and predicted specific attenuation over short-range mm-wave terrestrial links.

For rain attenuation over a short path at mm-wave frequencies, the effective rain rate that causes attenuation can be considerably higher than the rain cell's average rain intensity. Based on rain attenuations measured at 26 and 38 GHz in Malaysia, it has been found that the measured specific attenuation exceeds the expected value from ITU-R.838-3 by a factor of 1.8175. As previously assumed, the non-uniform distribution of the rain rate occurs due to the random temporal and spatial variations of rain which cause non-anomalous behaviour of specific attenuation and raindrops coalesce at d < 1 km. This leads to a heavier penalty in absorption and scattering processes [20].

In the next section, the increment factor proposed in [25] is utilised to interpret the increment trend of the specific attenuation γ_{eff} at mm-wave frequencies over a path length of less than 1 km.

4.1. Formulation of $I_{f\gamma}$

The distance factor r, proposed in [25], has been initially investigated. The increment factor of the rain rate $I_{f\gamma}$ in Eq. (12) should be equal to the reduction factor of Formula (13), expressed as follows:

$$I_{f\gamma} = \left[\frac{1}{0.477 d^{0.633}\, R_{0.01}^{0.073}\, f^{0.123}}\right] \text{for } f > 40\text{GHz},\ d < 1\text{km}, R_{0.01\%}, \geq 100\ (\text{mm}/\text{h}) \tag{13}$$

where the frequency is f in GHz, the rain rate at 0.01% is R0.01% in mm/hr and the path length is d in km. Fig. 11 presents $I_{f\gamma}$ as a function of its parameters from ITU-R P.530-17, as found in Formula (11) and proposed in Eq. (13), for 38 GHz in tropical and temperate climates [25]. The increment factor is inversely proportional to the path length, frequency and rain rate at one-minute integration time (d, R0.01% and f) when the signal propagates during rainfall events at R0.01% ≥ 100 (mm/h) and frequencies below 40 GHz. Fig. 11 indicates that ITU-R P.530-17 has the most consistent and predictive performance at longer distances (km), however, it overestimates the r factor at shorter

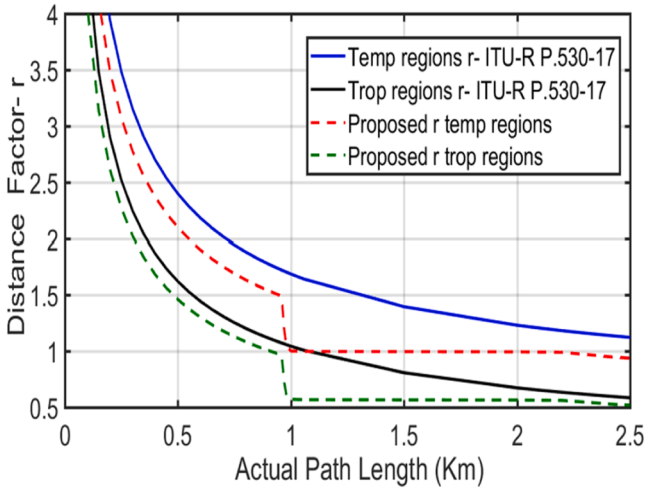

Fig. 11. Variations in reduction factor from ITU-R P.530-17, as found in Formula (11) and proposed in Eq. (13), for 38 GHz in tropical and temperate climates [25].

distances. In this method, r exponentially decreases up to 1 km and then slightly decreases for longer distances. It can be seen that the distance factor slightly decreases with increasing rain rates. Interestingly, the same observations were noted for long-term rain attenuation statistics conducted from September 2018 to September 2019 at 73 and 83 GHz for LOS links over 0.3 km in Malaysia [18,49].

The factor r significantly increases in temperate regions compared to tropical areas since the rain cell diameter is smaller for stratiform rain in temperate areas as opposed to the intense convective rain types in tropical regions [27]. At higher frequencies, the rain cell diameter must be considered more than the distance reduction factor. There is a strong correlation between the rainfall cell diameter at a given point and the signal attenuation at very short paths for mm-wave terrestrial links. This depends on the integration of the rainfall rate along a relatively short path length (100 m). The result from [50] confirms that heavy rainfall from convective clouds is a common phenomenon that frequently occurs in Malaysia. The study further verifies that a rain cell with a rain rate of 120 mm/h has a diameter of about 1.2–1.5 km. In comparison, temperate regions see rain cells measuring around 10 km for rates of 20 mm/h or more [46]. Thus, the size of the rain cell is defined by the distance covered. For tropical regions, the increment factor at frequencies above 40 GHz when R0.01% exceeds 100 mm/h can therefore be calculated (13).

The rain attenuation measured at 26 and 38 GHz in Malaysia is applied to optimise the expression of $I_{f\gamma}$, as given in Eq. (13). In the regression analysis, the sum square error R2 is 0.9721, which indicates the minimum error with measured data in the tropical region. The dependence of the increment factor on frequency is found to be negligible and therefore ignored in Eq. (13), as shown in Fig. 12. Hence, the increment factor for $f < 40$ GHz and d < 1 km is proposed as follows:

$$I_{f\gamma} = \left[\frac{1}{1.77 d^{0.77}\, R_{0.01}^{-0.05}}\right] f \leq 40\text{GHz and } d < 1\text{km} \tag{14}$$

where d is the short-range path length (<1 km) and R0.01% is the 1 min rain rate measured at 0.01%.

Fig. 11 demonstrates that the curve's trend and pattern are faster in tropical regions than in temperate areas. Mathematically, ($I_{f\gamma}$) is inversely proportional to the value of d, f and R0.01%. Hence, the increment factor of the rain rate ($I_{f\gamma}$) can be given, as presented in Eq. (13). When the increment factor of the rain rate ($I_{f\gamma}$) is analysed at different locations with temperate climates, it is shown to be inversely proportional to the square value of three parameters (d, f and R0.01%)

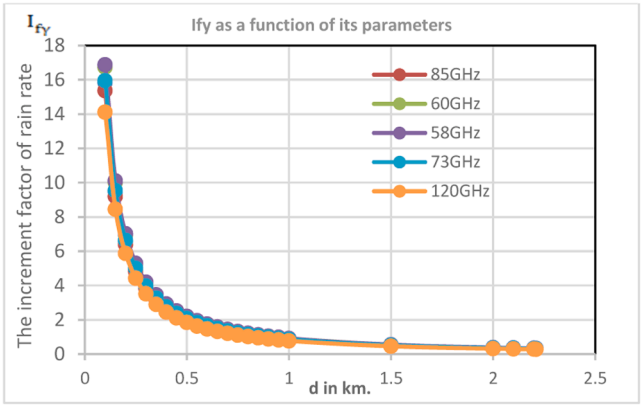

Fig. 12. $I_{f\gamma}$ as a function of its parameters for different frequencies and R0.01% =50mm\h for temperate climate areas.

when the rain rate < 100 mm/h and $f > 40$ GHz at a short path. Figs. 12 and 13 present $I_{f\gamma}$ for 75GHz measurement in Korea on a 100 m path length. Since it is inversely proportional to the square value of its parameters, the ($I_{f\gamma}$) can be written as:

$$I_{f\gamma} = \left[\frac{1}{0.477 d^{0.633} R_{0.01}^{0.073} f^{0.123}}\right]^2 \quad f > 40\text{GHz and } d < 1\text{km } R_{0.01\%} < 100 \text{ (mm/h} \tag{15}$$

Our observations indicate that the rain rate $R_{0.01\%}$ used by ITU-R does not represent the effective rain intensity-induced attenuation over mm-wave links less than 1 km path length, even though it is accurate for paths longer than 1 km. Therefore, the empirical formula to compute the effective rain rate R_{eff} is highly recommended to correct this underestimation of γ_{eff} in short paths based on physical link parameters.

5. Concept of effective rain rate (R_{eff})

New concepts and terms have introduced the "effective rain rate", defined as the peak value during the intersection between the rain cell and short path length. In [32], the concept of R_{eff} was introduced to prevent inconsistencies and maintain the general expression of R_{eff} without any changes. The concept of R_{eff} is briefly addressed by Yusuf et al. [30,48,51] where it is agreed that the rain rate exhibits inhomogeneity over short ranges. Measurement results indicate that power fluctuations are likely due to local variations in the rain rate occurring over distances significantly shorter than the overall path length (ranging from 265 m to 605 m) and moving across the line of sight during the sampling time. This observation aligns with conclusions from [52] which noted the short-term signal strength variations of up to 2–3 min during rain.

However, researchers have not calculated the effective rain rate induced attenuation over a short-range mm-wave terrestrial link. Thus, this paper proposes a new approach by considering the actual path length rather than just the d_{eff} and effective rain rate R_{eff}, as follows:

$$A_{0.01} = k\left[R_{eff}(R_{0.01};\ d)\right]^{\alpha} \times d \quad d < 1\text{km} \tag{16}$$

where R_{eff} is the effective rain rate, as a function of propagation path length shorter than 1 km d, and the rainfall rate exceeds 0.01% of the time $R_{0.01\%}$. The empirical formula that computes the effective rain rate R_{eff} is highly recommended to correct this underestimation of γ_{eff} in short path distances based on physical link parameters.

6. Modelling of effective rain rate and attenuation prediction

Based on Eq. (16), the effective specific attenuation can be expressed as:

$$\gamma_{eff} = k\, R_{eff}^{\alpha} = I_{f\gamma} \times \gamma = I_{f\gamma} \times k\, R_{0.01}^{\alpha} \tag{17.a}$$

$$\text{or } R_{eff} = \left[I_{f\gamma} \times R_{0.01}^{\alpha}\right]^{1/\alpha} \tag{17.b}$$

where the rain rate increment factor $I_{f\gamma}$ is calculated from Eqs. (13)–(15). The behaviour of R_{eff} with $R_{0.01\%}$ for various path length values at frequency 38 GHz is presented in Fig. 14. It is evident that when the link distance increases, the effective rain rate decreases, as observed in [39]. This result demonstrates that the peak of rain has a smaller cell size in any climatic region. Furthermore, the value of R_{eff} may be higher than $R_{0.01\%}$ for short propagation path lengths since high rain rates may dominate shorter path lengths at the centre of the rain cell [27].

Hence, the total attenuation for a path length less than 1 km, as proposed in (15), can be expressed as follows:

$$\begin{aligned} A_{0.01} &= \gamma_{eff} \times d \\ A_{0.01} &= k\left[R_{eff}\right]^{\alpha} \times d \end{aligned} \tag{18}$$

where R_{eff} can be obtained from (17.b) and k and α coefficient values can be obtained from ITU-R P.838-3. The value of $R_{0.01\%}$ can be acquired from local measurements or ITU-R P.837-7.

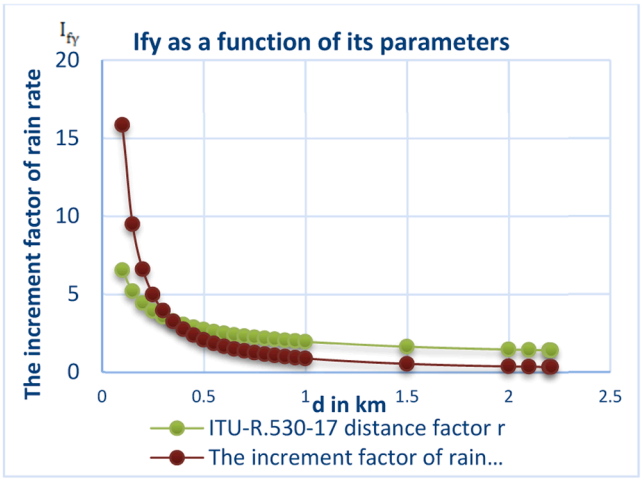

Fig. 13. $I_{f\gamma}$ as a function of its parameters from ITU-R P.530-17, as presented in Formula (11) and proposed in Eq. (13), at 75GHz and R0.01% =50mm\h for temperate climate areas.

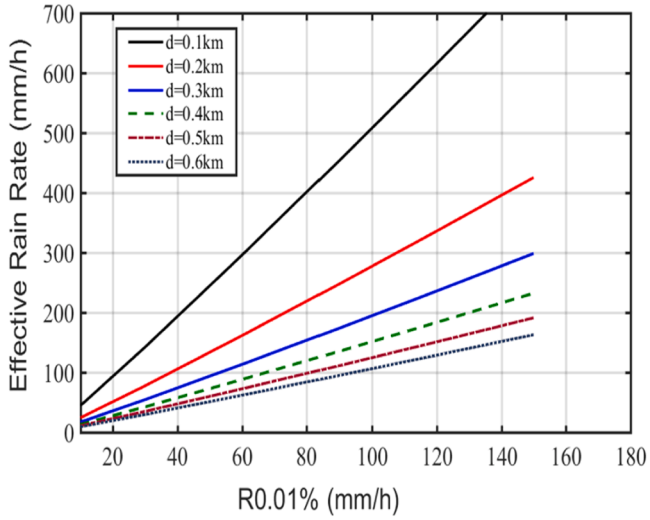

Fig. 14. Effective rain rate for 1-min rain rate at different distances <1 km.

6.1. Comparison of proposed model's estimations with measurements in Malaysia

Eqs. (13), (15), (17.b) and (18) are used to investigate the R_{eff} according to the measured terrestrial rain attenuation in Malaysia. A comparison is made between the CCDF of rain attenuation predicted by the proposed effective rain rate method and the experimental data at 26 and 38 GHz for 300 m path length, as presented in Fig. 15. Predictions by the proposed method are very similar to the measured rain attenuation at both frequencies. The measurements of rain attenuation statistics at 73.5GHz and 83.5GHz using LOS links were conducted in Malaysia from September 2018 to September 2019 over 0.3 km. The proposed model's predictions are further compared with real measurements [18,49]. As shown in Figs. 16–18, the proposed model's predictions are compared with the long-term measurements using E-Band links for all percentages of time in Malaysia. The increment factor of specific attenuation I_{f_γ} is 1.8149 at R0.01%, which corresponds to a rain rate of 144 mm/h. Whereas at 26GHz and 38 GHz, I_{f_γ} is 1.8175 which corresponds to a rain rate of 125 mm/h. Figs. 16 and 17 indicate that the proposed R_{eff} and rain rate data in [18–49] are very similar throughout all percentages of time.

The shape of the CCDF curves does not change with the application of effective rain rate, and the proposed empirical model's attenuation is in excellent agreement with the measured attenuation. It can be seen that rain attenuation at both 73.5GHz and 83.5GHz using E-band links and calculated by the effective rain concept are comparable at a range of 20–25 dB over 300 m. The maximum value of rain attenuation (almost 25 dB using E-band links) occurs when the rain rate is at a maximum (nearly 193 mm/h), which corresponds to 0.001% of time. It is noteworthy that the proposed model performs better at R0.001% ($0.001 \leq P \leq 1$). The prediction errors are in the range of 0.69–0.96 dB at low rain rates (when $p \geq 0.01\%$) and at a range of 0.03–0.17 dB (when $p \leq 0.01\%$) depending on the link frequency. From the analyses, it is clear that the deviations of rain fade at very short paths AP% dB can be related to the rainfall rate RP% exceeded at %P [43] (Fig. 18).

6.2. Validation of the proposed model at different climatic regions

As illustrated in Fig. 19, the proposed model can predict at 25GHz measurement in Japan and 75GHz measurement in Korea for 223 m, 150 m and 100 m path lengths, respectively. Based on a comparison between the experimental results presented in Figs. 10 and 11, it is evident that the concept of effective rain rate over the short-range millimetre-wave terrestrial link has produced reliable prediction with separate frequencies at different paths and locations. Thus, the effective rain rate

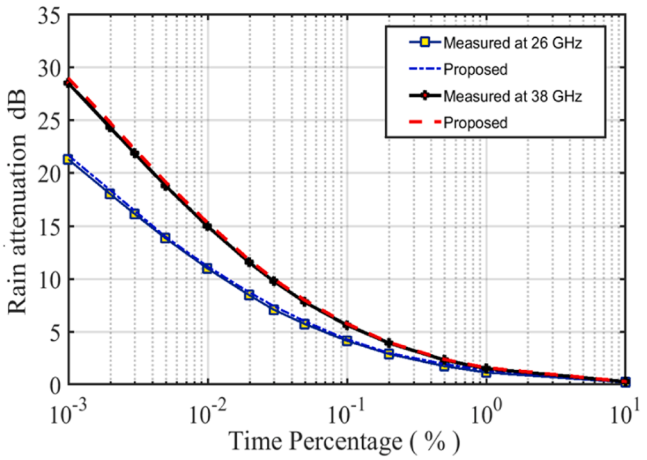

Fig. 15. Comparison between measured and predicted rain attenuation in Malaysia using R_{eff} technique at $F < 40$ GHz over 300 m.

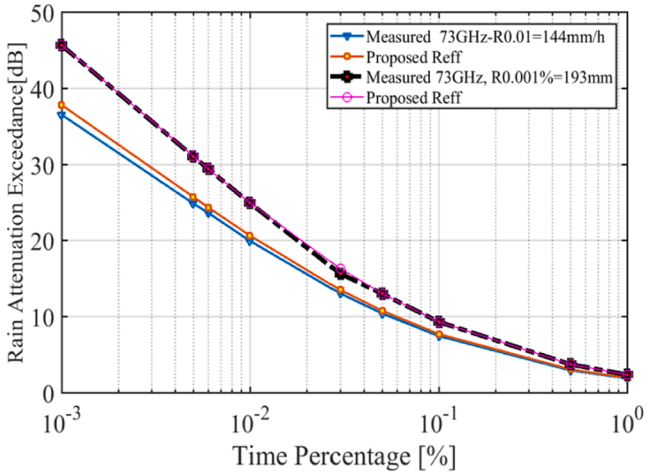

Fig. 16. Comparison between measured and predicted rain attenuation in Malaysia using R_{eff} technique at 73 GHz over 300m, $R_p, > 100$ $\left(\frac{mm}{h}\right)$.

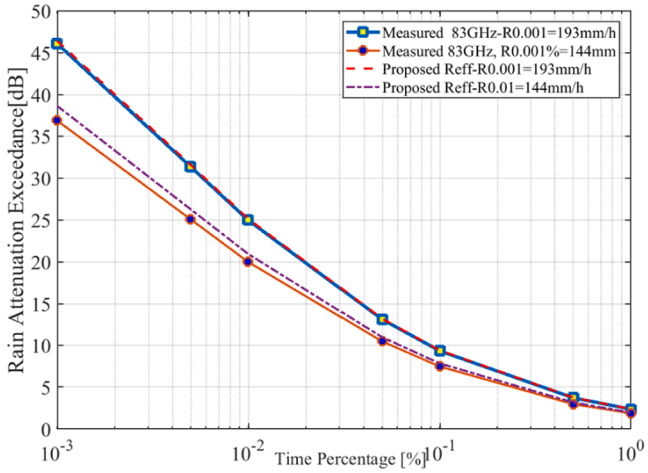

Fig. 17. Comparison between measured and predicted rain attenuation in Malaysia using R_{eff} technique at 83 GHz over 300m, $R_p, > 100$ $\left(\frac{mm}{h}\right)$.

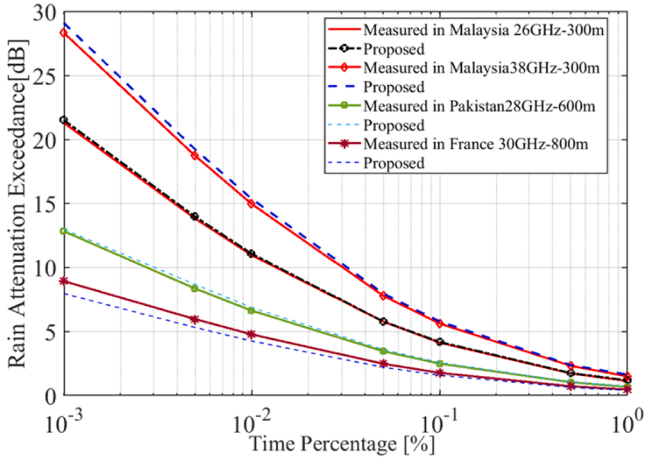

Fig. 18. Comparison between measured and predicted rain attenuation using the R_{eff} technique for frequencies <40 GHz over path length <1 km at different geographical locations.

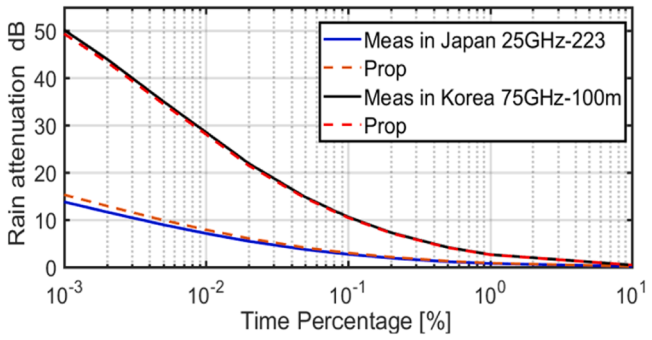

Fig. 19. Comparison between measured rain attenuation CCDF with those predicted by the proposed modified model at 25GHz for 223 m in Japan and 75GHz for 100 m in Korea.

can interpret the increase of effective specific attenuation over paths less than 700 m.

For further validations, the proposed model was used to transform one-minute rain attenuation data to effective rain rate over short paths in other geographical locations, such as Japan [54,53], Korea [35,47], Spain [38], New Mexico [59], France [55], USA [52], Pakistan [56] and Prague [57]. The effective rain rate seems fairly reasonable, with slight prediction errors at path length <700 m due to different propagation characteristics, such as one-minute rain rate cell size and frequency band. Therefore, the conversion technique provides a relatively accurate method for predicting attenuation at millimetre-wave frequencies over short path lengths in Malaysia and for different climates, as shown in Fig. 20.

7. Prediction error estimation

Performance evaluation has been accomplished by analysing the discrepancies between the model's predictions and the databank values while assessing the model's accuracy, robustness and reliability. Testing metrics and criteria include statistical measures such as root mean square error (RMSE), mean absolute error (MAE) and coefficient of determination (R-squared) [58,60,61]. The documentation serves as a record of the testing process and can be used for model validation, regulatory compliance or communication with stakeholders. The Root Mean Square Error values are calculated for the available rain attenuation studies using mm-waves and short path length at different regions worldwide to validate the proposed model. From Eqs. (17) and (18), it is clear that the results obtained from the proposed method provides a higher prediction accuracy with low RMSE values at 0.107 for both frequencies (higher and lower than 40 GHz) in different climate regions with the mean absolute percentage error MAPE at 3.76%. The RMSE values for short path links working at frequency bands > 40 GHz are 0.018 less than the RMSE values for short path links working at frequency bands < 40 GHz, which is 0.179. It is worth noting that the proposed model performs better in predicting rain attenuation over short range terrestrial links working at millimetre-wave frequencies higher than 40 GHz in different climatic regions.

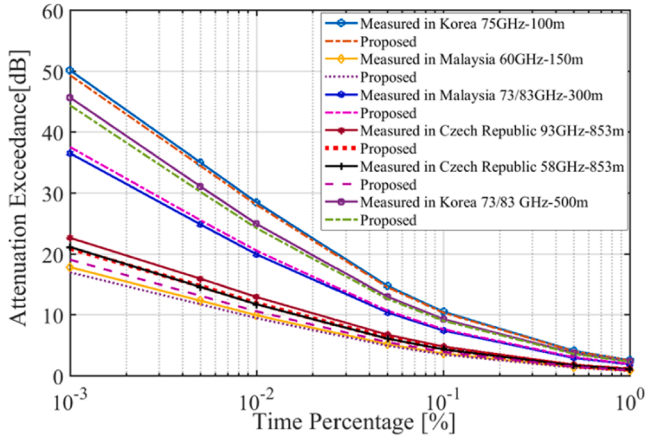

Fig. 20. Comparison between measured and predicted rain attenuation using R_{eff} technique for frequencies >40 GHz and path length <1 km at different geographical locations.

$$\mathrm{RMSE} = \sqrt{\sum_{i=1}^{k} \frac{(\mathrm{Am} - \mathrm{Ap})^2}{k}} \tag{19}$$

$$\mathrm{MAPE} = \frac{100\%}{k} \sum_{i=1}^{k} \frac{|\mathrm{Am} - \mathrm{Ap}|}{\mathrm{Am}} \tag{20}$$

8. Conclusion

Two-year measurements of both the rain rate and rain-induced attenuation over two experimental terrestrial links operating at 26 and 38 GHz at 0.3 km path length in Malaysia have been investigated. Significant discrepancies are present between the measured attenuation induced by rain and the one predicted by ITU-R. P.530-17. Several recent observations indicate that the rain rate at 0.01% occurrence ($R_{0.01\%}$) used by the ITU-R prediction method does not represent the effective rain intensity for less than 1 km path length, even though it is accurate for paths longer than 1 km. As the rain rate increases, the rain rate distribution becomes increasingly non-uniform, even at a very short path length. This paper introduced an effective rain rate (R_{eff}) concept modelled to eliminate the need for effective path lengths for short links, representing the variations of rain intensities over a very short path. The proposed effective rain rate (R_{eff}) was developed based on the measured R0.01% and short-range path length (less than 1 km). The proposed model estimates have been validated and improved using the measurements for long-term rain attenuation statistics (conducted from September 2018 to September 2019) at 73.5GHz and 83.5GHz over 0.3 km in Malaysia. Available measurements of 25GHz on 223 m paths in Japan and 75GHz on 100 m paths in Korea have also been validated. The proposed effective rain estimations were compared with direct measurements from several different climates. Therefore, the effective rain rate technique provides a relatively accurate method for predicting the attenuation at millimetre-wave frequencies over short path lengths in Malaysia and other environments. The proposed model has achieved very high accuracy over communication path lengths ranging from 100 m to 600 m. The effective rain rate seems relatively reasonable, with slight prediction errors at path length >700 m due to different propagation characteristics, such as one-minute rain rate cell size and frequency band. Hence, the proposed effective rain rate model is recommended for path loss calculations and channel design in outdoor applications over mm-wave links at short paths.

CRediT authorship contribution statement

Asma Ali Budalal: Writing – review & editing, Writing – original draft, Visualization, Validation, Software, Project administration, Methodology, Investigation, Formal analysis. **Ibraheem Shayea:** Writing – review & editing, Project administration. **Md. Rafiqul Islam:** Resources, Funding acquisition, Data curation. **Jafri Din:** Resources. **Abdulsamad Ebrahim Yahya:** Writing – review & editing. **Yousef Ibrahim Daradkeh:** Writing – review & editing. **Marwan Hadri Azmi:** Conceptualization.

Declaration of competing interest

The authors certify that they have no affiliations or involvement with

any organization or entity that has a financial interest (including honoraria, educational grants, participation in speakers' bureaus, memberships, employment, consultancies, stock ownership, or other equity interests; as well as expert testimony or patent-licensing arrangements), or a non-financial interest (including personal or professional relationships, affiliations, knowledge, or beliefs) related to the subject matter or materials discussed in this manuscript.

The authors report the following affiliations or involvement with organizations or entities that may have a financial or non-financial interest in the subject matter or materials discussed in this manuscript. Please specify the nature of the conflict on a separate sheet if additional space is required.

Acknowledgments

This work is supported by the Department of Electrical and Computer Engineering, International Islamic University Malaysia (IIUM), Gombak, 5072 Malaysia and the College of Electrical & Electronics Technology - Benghazi, Libya. Also, this research study was sponsored by the Higher Institution Centre of Excellence (HICOE) program, Ministry of Higher Education (MOHE) Malaysia, conducted at the Universiti Teknologi Malaysia under the HiCOE Research Grant R.J130000.7823.4J637 and R.J130000.7823.4J642.

Data availability

The data that has been used is confidential.

References

[1] M. Xiao, S. Mumtaz, Y. Huang, L. Dai, Y. Li, M. Matthaiou, et al., Millimeter wave communications for future mobile networks, IEEE J. Sel. Areas Commun. 35 (2017) 1909–1935.
[2] C. Han, S. Duan, Impact of atmospheric parameters on the propagated signal power of millimeter-wave bands based on real measurement data, IEEE Access 7 (2019) 113626–113641.
[3] W. Hong, Z.H. Jiang, C. Yu, D. Hou, H. Wang, C. Guo, Y. Hu, L. Kuai, Y. Yu, Z. Jiang, Z. Chen, The role of millimeter-wave technologies in 5G/6G wireless communications, IEEE J. Microw. 1 (1) (2021) 101–122.
[4] N. Heuveldop, Ericsson mobility report, Ericsson, Stockholm, 2017.
[5] Agenda and Reference (Resolutions and Recommendations), ITU. August 2017. Available online: https://www.itu.int/dms_pub/itu-r/oth/14/02/R14020000010001PDFE.pdf (accessed on 31 January 2020).
[6] J.M. Molina-García-Pardo, L. Rubio, M.T. Martinez-Inglés, E. Egea-Lopez, A. Mateo-Aroca, V.M.R. Peñarrocha, J. Reig, Wireless channel characterization from 2 to 28 GHz in an outdoor parking lot, IEEE Antennas Wirel. Propag. Lett. (2024).
[7] D. Shakya, S. Ju, O. Kanhere, H. Poddar, Y. Xing, T.S. Rappaport, Radio propagation measurements and statistical channel models for outdoor urban microcells in open squares and streets at 142, 73, and 28 GHz, IEEE Trans. Antennas Propag. (2024).
[8] T.S. Rappaport, et al., Millimeter wave mobile communications for 5G cellular: it will work!, IEEE Access 1 (2013) 335–349.
[9] J.F. Federici, J. Ma, L. Moeller, Review of weather impact on outdoor terahertz wireless communication links, Nano Commun. Netw. 10 (Dec. 2016) 13–26.
[10] P. Sen, et al., Terahertz communications can work in rain and snow: impact of adverse weather conditions on channels at 140 GHz, in: Proceedings of the 6th ACM Workshop on Millimeter-Wave and Terahertz Networks and Sensing Systems, 2022, pp. 13–18.
[11] A.A. Budalal, M.R. Islam, Path loss models for outdoor environment—With a focus on rain attenuation impact on short-range millimeter-wave links, e Prime Adv. Electr. Eng. Electron. Energy 3 (2023) 100106.
[12] A. Hilt, Microwave hop-length and availability targets for the 5g mobile backhaul, in: Proceedings of the 2019 42nd International Conference on Telecommunications and Signal Processing (TSP), 2019, pp. 187–190.
[13] S. Nandi and D. Nandi, "Comparative study of rain attenuation effects for the design of 5G millimeter wave communication between tropical and temperate region," in 2017 Devices For Integrated Circuit (DevIC), 2017, pp. 747–750.
[14] H. Lam, L. Luini, J. Din, M. Alhilali, S. Jong, F. Cuervo, Impact of rain attenuation on 5G millimeter wave communication systems in equatorial Malaysia investigated through disdrometer data, in: Proceedings of the 2017 11th European Conference on Antennas and Propagation (EUCAP), 2017, pp. 1793–1797.
[15] D. Nandi, A. Maitra, The effects of rain on millimeter wave communication for tropical region, in: Proceedings of the 2019 URSI Asia-Pacific Radio Science Conference (AP-RASC), 2019, pp. 1–3.
[16] I. Shayea, T. Abd. Rahman, M. Hadri Azmi, A. Arsad, Rain attenuation of millimetre wave above 10 GHz for terrestrial links in tropical regions, Trans. Emerg. Telecommun. Technol. 29 (2018) e3450.
[17] A.A. Budalal, I.M. Rafiqul, M.H. Habaebi, T.A. Rahman, The effects of rain fade on millimetre wave channel in tropical climate, Bull. Electr. Eng. Inform. 8 (2019) 653–664.
[18] A.M. Al-Saman, M. Cheffena, M. Mohamed, M.H. Azmi, Y. Ai, Statistical analysis of rain at millimeter waves in tropical area, IEEE Access 8 (2020) 51044–51061.
[19] A. De, A. Maitra, Dependence of rain attenuation on rain rate and drop size distribution for ka-band satellite communication over India, Adv. Space Res. (2024).
[20] S.K. Kotamraju, C.S.K. Korada, Precipitation and other propagation impairments effects at microwave and millimeter wave bands: a mini survey, Acta Geophys. 67 (2019) 703–719.
[21] M. Alhilali, J. Din, M. Schonhuber, H.Y. Lam, Estimation of millimeter wave attenuation due to rain using 2d video distrometer data in malaysia, Indones. J. Electr. Eng. Comput. Sci. 7 (2017) 164–169.
[22] P. Kántor, J. Bitó, Á. Drozdy, Characteristics of 5G wireless millimeter wave propagation: transformation of rain attenuation applying different prediction models, in: Proceedings of the 2016 10th European Conference on Antennas and Propagation (EuCAP), 2016, pp. 1–5.
[23] T.S. Rappaport, F. Gutierrez, E. Ben-Dor, J.N. Murdock, Y. Qiao, J.I. Tamir, Broadband millimeter-wave propagation measurements and models using adaptive-beam antennas for outdoor urban cellular communications, IEEE Trans. Antennas Propag. 61 (2012) 1850–1859.
[24] A.A. Budalal, M.R. Islam, M.H. Habaebi, T.A. Rahman, Millimeter wave channel modeling–Present development and challenges in tropical areas, in: Proceedings of the 2018 7th International Conference on Computer and Communication Engineering (ICCCE), 2018, pp. 23–28.
[25] A.A.H. Budalal, M.R. Islam, K. Abdullah, T.A. Rahman, Modification of distance factor in rain attenuation prediction for short-range millimeter-wave links, IEEE Antennas Wirel. Propag. Lett. 19 (2020) 1027–1031.
[26] A.A. Budalal, I. Shayea, M.R. Islam, M.H. Azmi, H. Mohamad, S.A. Saad, Y. I. Daradkeh, Millimetre-wave propagation channel based on NYUSIM channel model with consideration of rain fade in tropical climates, IEEE Access 10 (2021) 1990–2005.
[27] P.O. Akuon, Rain cell ratio technique in path attenuation for terrestrial radio links, Int. J. Electron. Commun. Eng. 13 (2019) 403–411.
[28] J. Huang, Y. Cao, X. Raimundo, A. Cheema, S. Salous, Rain statistics investigation and rain attenuation modeling for millimeter wave short-range fixed links, IEEE Access 7 (2019) 156110–156120.
[29] L. Luini, G. Roveda, M. Zaffaroni, M. Costa, C.G. Riva, The impact of rain on short {E} -band radio links for 5G mobile systems: experimental results and prediction models, IEEE Trans. Antennas Propag. 68 (2019) 3124–3134.
[30] A.A. Yusuf, A. Falade, B. Olufeagba, O. Mohammed, T.A. Rahman, Statistical evaluation of measured rain attenuation in tropical climate and comparison with prediction models, J. Microw. Optoelectron. Electromagn. Appl. 15 (2016) 123–134.
[31] R. Ghiani, L. Luini, A. Fanti, A physically based rain attenuation model for terrestrial links, Radio Sci. 52 (2017) 972–980.
[32] L.A.R.D.S. Mello, M.S. Pontes, Prediction of rain attenuation in terrestrial links with the full rainfall rate distribution, in: Proceedings of the IET Conference, 2007, p. 748. -748Available, https://digital-library.theiet.org/content/conferences/10.1049/ic.2007.0872.
[33] RECOMMENDATION ITU-R P.838-3, Specific attenuation model for rain for use in prediction methods, International Telecommunication Union, 2005.
[34] ITU-R. Propagation Data and Prediction Methods Required for the Design of Terrestrial Line-of-Sight 17, Systems P Series Radiowave Propagation, 2017.
[35] S. Shrestha, D.Y. Choi, Rain attenuation statistics over millimeter wave bands in South Korea, J. Atmos. Sol. Terr. Phys. 152 (2017) 1–10.
[36] I. Shayea, L.A. Nissirat, M.A. Nisirat, A. Alsamawi, T. Abd. Rahman, M. Hadri Azmi, et al., Rain attenuation and worst month statistics verification and modeling for 5G radio link system at 26 GHz in Malaysia, Trans. Emerg. Telecommun. Technol. 30 (2019) e3697.
[37] P. Valtr, P. Pechač, On distance factor in rain attenuation predictions, in: Proceedings of the 2019 13th European Conference on Antennas and Propagation (EuCAP), 2019, pp. 1–3.
[38] J.M. García-Rubia, J.M. Riera, P. Garcia-del-Pino, A. Benarroch, Attenuation measurements and propagation modeling in the W-band, IEEE Trans. Antennas Propag. 61 (2012) 1860–1867.
[39] F. Norouzian, E. Marchetti, M. Gashinova, E. Hoare, C. Constantinou, P. Gardner, et al., Rain attenuation at millimeter wave and low-THz frequencies, IEEE Trans. Antennas Propag. 68 (2019) 421–431.
[40] P. Valtr, M. Fencl, V. Bareš, Excess attenuation caused by antenna wetting of terrestrial microwave links at 32 GHz, IEEE Antennas Wirel. Propag. Lett. 18 (2019) 1636–1640.
[41] M. Islam, A. Tharek, J. Din, J. Chebil, Measurement of wet antenna effects on microwave propagation-an analytical approach, in: Proceedings of the 2000 Asia-Pacific Microwave Conference, 2000, pp. 1547–1551 (Cat. No. 00TH8522).
[42] E. Alozie, A. Abdulkarim, I. Abdullahi, A.D. Usman, N. Faruk, I.F.Y. Olayinka, L. S. Taura, A review on rain signal attenuation modeling, analysis and validation techniques: advances, challenges and future direction, Sustainability 14 (18) (2022) 11744.
[43] A. Abdulrahman, T.A. Rahman, B. Olufeagba, M.R. Islam, Using full rainfall rate distribution for rain attenuation predictions over terrestrial microwave links in Malaysia, Signal Process. Res. 2 (2013) 25–28.

[44] F. Nauval, H. Hashiguchi, Regional and diurnal variations of rain attenuation obtained from measurement of raindrop size distribution over Indonesia at ku, ka and W bands, Prog. Electromagn. Res. 57 (2017) 25–34.
[45] M.M. Hasan, R. Jayawardene, T. Hirano, J. Hirokawa, M. Ando, Localisation of rain and its effect on propagation in Tokyo tech millimeter-wave model network, in: Proceedings of the International Symposium on Antennas and Propagation, 2011, pp. 26–28.
[46] S. Begum, I.E. Otung, Rain cell size distribution inferred from rain gauge and radar data in the UK, Radio Sci. 44 (2009) 1–7.
[47] J.H. Kim, M.W. Jung, Y.K. Yoon, Y.J. Chong, The measurements of rain attenuation for terrestrial link at millimeter wave, in: Proceedings of the 2013 International Conference on ICT Convergence (ICTC), 2013, pp. 848–849.
[48] S. Shrestha, D.Y. Choi, Rain attenuation study over an 18 GHz terrestrial microwave link in South Korea, Int. J. Antennas Propag. 2019 (2019) 1–16.
[49] A. Al-Saman, M. Mohamed, M. Cheffena, M.H. Azmi, T.A. Rahman, Performance of full-duplex wireless backhaul link under rain effects using E-Band 73 GHz and 83 GHz in tropical area, Appl. Sci. 10 (2020) 6138.
[50] N.H.H. Khamis, J. Din, T.A. Rahman, Determination of rain cell size distribution for microwave link design in Malaysia, in: Proceedings of the 2004 RF and Microwave Conference, IEEE, 2004, pp. 38–40. Cat. No. 04EX924.
[51] A.Y. Abdulrahman. Development of terrestrial rain attenuation transformation model for slant-path attenuation predictions in tropical regions. A thesis submitted in fulfilment of the requirements for the award of the degree of Doctor of Philosophy (Electrical Engineering) at Faculty of Electrical Engineering, Universiti Teknologi, Malaysia, 2012.
[52] H. XU. Terrestrial radio wave propagation at millimeter-wave frequencies, Virginia Polytechnic Institute and State University, 2000. PhD Thesis.
[53] A. Hirata, R. Yamaguchi, H. Takahashi, T. Kosugi, K. Murata, N. Kukutsu, et al., Effect of rain attenuation for a 10-Gb/s 120-GHz-band millimeter-wave wireless link, IEEE Trans. Microw. Theory Tech. 57 (2009) 3099–3105.
[54] W. Chujo, T. Manabe, S.I. Yamamoto, 60-GHz short-range terrestrial rainfall attenuation compared with K-band long-distance satellite link, in: Proceedings of the 2014 International Symposium on Antennas and Propagation Conference Proceedings, 2014, pp. 559–560.
[55] O. Veyrunes, P. Le Clerc, H. Sizun, First results of precipitation effects at 30, 50, 60 and 94 GHz on a 800 m link in Belfort (France), 1999, pp. 77–80.
[56] U. Korai, L. Luini, R. Nebuloni, I. Glesk, Statistics of attenuation due to rain affecting hybrid FSO/RF link: application for 5G networks, in: Proceedings of the 2017 11th European Conference on Antennas and Propagation (EUCAP), 2017, pp. 1789–1792.
[57] V. Kvicera, M. Grabner, O. Fiser, Comparison of hydrometeor attenuation on parallel terrestrial paths at 58 GHz and 93 GHz, in: Proceedings of the 2011 XXXth URSI General Assembly and Scientific Symposium, 2011, pp. 1–4.
[58] D. Chicco, M.J. Warrens, G. Jurman, The coefficient of determination R-squared is more informative than SMAPE, MAE, MAPE, MSE and RMSE in regression analysis evaluation, Peerj Comput. Sci. 7 (2021) e623.
[59] E. Hong, S. Lane, D. Murrell, N. Tarasenko, C. Christodoulou, Terrestrial link rain attenuation measurements at 84 GHz, in: Proceedings of the 2017 United States National Committee of URSI National Radio Science Meeting (USNC-URSI NRSM), 2017, pp. 1–2.
[60] D. Chicco, M.J. Warrens, G. Jurman, The coefficient of determination R-squared is more informative than SMAPE, MAE, MAPE, MSE and RMSE in regression analysis evaluation, Peerj Comput. Sci. 7 (2021) e623.
[61] J.O. Afape, A.A. Willoughby, M.E. Sanyaolu, O.O. Obiyemi, K. Moloi, J.O. Jooda, O.F. Dairo, Improving millimetre-wave path loss estimation using automated hyperparameter-tuned stacking ensemble regression machine learning, Results Eng. 22 (2024) 102289. VolumeISSN 2590-1230.